

ChemComm

Accepted Manuscript



This article can be cited before page numbers have been issued, to do this please use: X. Liu, S. Cui, M. Qian, Z. Sun and P. Du, *Chem. Commun.*, 2016, DOI: 10.1039/C6CC00526H.



This is an *Accepted Manuscript*, which has been through the Royal Society of Chemistry peer review process and has been accepted for publication.

Accepted Manuscripts are published online shortly after acceptance, before technical editing, formatting and proof reading. Using this free service, authors can make their results available to the community, in citable form, before we publish the edited article. We will replace this *Accepted Manuscript* with the edited and formatted *Advance Article* as soon as it is available.

You can find more information about *Accepted Manuscripts* in the [Information for Authors](#).

Please note that technical editing may introduce minor changes to the text and/or graphics, which may alter content. The journal's standard [Terms & Conditions](#) and the [Ethical guidelines](#) still apply. In no event shall the Royal Society of Chemistry be held responsible for any errors or omissions in this *Accepted Manuscript* or any consequences arising from the use of any information it contains.



Journal Name

COMMUNICATION

In Situ Generated Highly Active Copper Oxide Catalyst for Oxygen Evolution Reaction at Low Overpotential in Alkaline Solutions

Xiang Liu, Shengsheng Cui, Manman Qian, Zijun Sun, Pingwu Du*

Received 00th January 20xx,
Accepted 00th January 20xx

DOI: 10.1039/x0xx00000x

www.rsc.org/

Developing efficient water oxidation catalysts made of earth-abundant elements has attracted much attention as a step toward for future clean energy production. Herein we report a simple one-step method to generate a low cost copper oxide catalyst film in situ from copper(II) ethylenediamine complex. The resulting catalyst has excellent activity toward oxygen evolution reaction in alkaline solutions. A catalytic current density of 1.0 mA/cm² and 10 mA/cm² for the catalyst film requires the overpotentials of only ~370 mV and ~475 mV in 1.0 M KOH, respectively. This catalytic performance shows that the new catalyst is one of the best Cu-based heterogeneous OER catalysts to date.

Conversion of electricity or solar energy into chemical fuels via water splitting is a great challenge and the design of highly efficient and low cost catalysts for oxygen evolution reaction (OER) has attracted great attention.¹⁻³ OER catalysis is a four-electron transfer process coupled with the removal of four protons from water molecules, which is much more complicated and difficult than water reduction reaction for hydrogen (H₂) production. Therefore, an efficient OER half-reaction might be the key to achieve high-performance water splitting for H₂ production.⁴⁻⁶ This point has led to a high demand for highly active materials for OER catalysis. Inspired by nature, many catalysts with structure and/or function similar to Mn cluster have been designed to realize water oxidation under moderate overpotentials, including well-known Ru- and Ir-based catalysts.⁷⁻⁸ More recently, much attention has been focused on low-cost catalysts based on first-row transition metals such as manganese,^{5,9} cobalt (Co),^{2,10-11} nickel (Ni),¹² copper (Cu),¹³⁻¹⁵ and iron (Fe).¹⁶

Cu is a very attractive element for catalysis because of its high abundance and low cost, which is even cheaper than Co and Ni. In addition, Cu plays a key role as the active metal center in a series of enzymes, such as copper monooxygenases, cytochrome C oxidases and other enzymes. The reduction of Cu^{II} to Cu^I/Cu⁰ and oxidation to Cu^{III} provides Cu^{II} with well-defined coordination chemistry and

extensive redox properties.¹⁷⁻²⁰ Thus, Cu-based catalysts have great potential in energy applications.

Recently, our group reported that heterogeneous copper oxide is active for water oxidation,²¹ and that the catalytic activities of the heterogeneous Cu-based catalysts can be tuned by the morphologies and sizes in CuO nanomaterials.²² We later found that Cu(OH)₂ is one of the active species for water oxidation during electrodeposition.²³ In addition, a few other groups also reported that CuO or Cu-Bi is an active catalyst for OER catalysis.²⁴⁻²⁵ Although much progress has been achieved to explore the Cu-based catalytic systems for OER (Table 1), all of the above-mentioned catalysts still showed lower catalytic activities than cobalt- or nickel-based catalysts such as mesoporous Co₃O₄ (overpotential, η ~410 mV for 10 mA/cm²),²⁶ Co-Pi (η ~410 mV for 1.0 mA/cm²),¹⁰ Co NPs (η ~390 mV for 10 mA/cm²),²⁷ Ni-Bi (η ~430 mV for 1.0 mA/cm²),²⁸ and Ni₂P (η ~400 mV for 10 mA/cm²),²⁹. Therefore, it is highly desirable to search for efficient Cu-based catalysts with highly improved performance, which are comparable to the well-known cobalt- or nickel-based catalysts for OER.

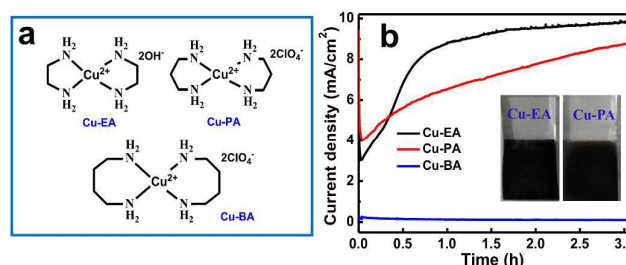


Figure 1. (a) Molecular structures of the Cu-EA, Cu-PA, and Cu-BA complexes. (b) Catalytic current densities for bulk electrolysis at 0.8 V (vs. Ag/AgCl) in 0.1 M KOH solution containing 3.0 mM Cu-EA (black), Cu-PA (red), and Cu-BA (blue) using FTO as the working electrode at pH 13.0.

In this present study, we demonstrate that a heterogeneous Cu-based catalyst that is highly active in alkaline solutions can be generated in situ from simple copper(II) ethylenediamine (Cu-EA) and copper(II) 1,3-propanediamine (Cu-PA) complexes (Figure 1a). In addition, the catalyst exhibited excellent robustness for catalytic oxygen evolution in 1.0 M KOH and the required overpotentials are only ~370 mV and ~475 mV to achieve a current density of 1.0 mA/cm² and 10 mA/cm², respectively. These overpotentials for water oxidation, to the best of our knowledge, are better than all

Key Laboratory of Materials for Energy Conversion, Chinese Academy of Sciences, Department of Materials Science and Engineering, iChEM(Collaborative Innovation Center of Chemistry for Energy Materials), University of Science and Technology of China (USTC), 96 Jinzhai Road, Hefei, Anhui Province, 230026, P. R. China. Email: dupingwu@ustc.edu.cn; Fax: 86-551-63606207.

Electronic Supplementary Information (ESI) available: See
DOI: 10.1039/x0xx00000x

the reported Cu-based heterogeneous catalysts for water oxidation. The catalyst material was extensively studied by scanning electron microscopy (SEM), X-ray photoelectron spectroscopy (XPS), and powder X-ray diffraction (XRD).

Initially, three copper complexes **Cu-EA**, **Cu-PA**, and **Cu-BA** were used as the catalysts for water oxidation catalysis. Bulk electrolysis (BE) experiments using a bare FTO electrode as the working electrode were performed in a 0.1 M KOH solution (pH ~13) containing 3.0 mM different copper complexes. A Pt wire was used as the counting electrode and an Ag/AgCl (3 M KCl) electrode was utilized as the reference electrode. As shown in Figure 1b, the catalytic current density in **Cu-EA** solution rapidly increased under an applied potential of 0.8 V vs. Ag/AgCl in the first hour. A large amount of gas bubbles appeared on the surface of the electrode. The gas was confirmed to be oxygen by both gas chromatography and a fluorescence-based oxygen sensor, indicating that water oxidation catalysis had occurred in this conditions. After long-term electrolysis for 3 h, the catalytic current density impressively reached ~10 mA/cm² and a black-gray thin film was clearly observed on the FTO electrode (see the inset picture in Figure 1b), suggesting the **Cu-EA** complex probably served as the active catalyst precursor for water oxidation.

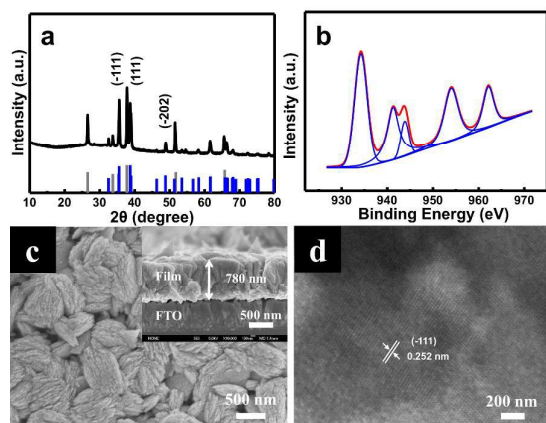


Figure 2. (a) Powder XRD patterns, (b) high resolution XPS spectrum of Cu 2p, (c) SEM image, and (d) high resolution TEM image of electrodeposited CuO material obtained from **Cu-EA**. Inset: the cross-sectional SEM image of the catalyst thin film on FTO plate.

Continuous cyclic voltammogram (CV) scans using 3.0 mM **Cu-EA** complex in 0.1 M KOH showed consistent results with increasing catalytic current density (Figure S1), further confirming the formation of heterogeneous active catalyst on the FTO electrode. In Figure S1, the initial CV scan between 0 and 0.8 V vs. Ag/AgCl at a scan rate of 100 mV shows obvious catalytic potential after ~0.6 V. With continuous CV scans for 1000 cycles, the catalytic onset potentials for water oxidation significantly decreased from ~0.6 V to ~0.5 V vs. Ag/AgCl. Meanwhile, the catalytic current density was highly enhanced. For example, the corresponding value increased from 0.8 mA/cm² to 5.7 mA/cm² at 0.8 V. As before, a black thin film was observed on the FTO during continuous CV scans and obvious oxygen gas bubbles were generated.

When using the **Cu-PA** complex to replace **Cu-EA** in solution to perform the BE experiment under the same conditions (red plot in Figure 1b), similar black-gray thin film was generated during electrodeposition, while a lower current density of 8.5 mA/cm² was achieved after 3 hours for electrolysis. When using **Cu-BA** complex,

the catalytic performance was much worse than either of the other complexes (blue plot in Figure 1b). No obvious catalytic film could be seen and the current density remained as low as 0.1 mA/cm² for 3 hours. Obvious blue Cu(OH)₂ precipitate was observed at the bottom of the electrochemical cell, indicating that **Cu-BA** complex is not stable in such a strong alkaline solution and the complex decomposed to form Cu(OH)₂. Therefore, among these three copper complexes, only **Cu-EA** and **Cu-PA** can be used as good precursors to generate active copper-based heterogeneous catalyst in 0.1 M KOH for water oxidation. Since the **Cu-EA** complex precursor showed the better catalytic activity, it was then chosen for the subsequent catalytic studies.

To provide more insights into the heterogeneous catalyst generated in situ from **Cu-EA** solution, the material was characterized by powder X-ray diffraction (XRD), as shown in Figure 2a. The diffraction patterns of the material on the FTO electrode were sharp and can be ascribed to typical CuO diffraction character (PDF#89-5895) and the SnO₂ character on the FTO substrate (PDF#46-1088). No other impurity peak can be observed. These results indicate high crystallinity and good purity of the electrodeposited CuO catalyst materials. The main crystalline peaks of the catalyst were located at the (-111) and (111) phases.

Table 1. Copper-based heterogeneous catalysts for OER

Catalyst	η (mV vs 1.0 mA/cm ²)	η (mV vs 10 mA/cm ²)	Refs.
CuO from Cu-TPA	600	--	26
Cu-bifunctional	749	--	28
CuO nanowires	550	--	27
Cu-Bi	530	--	29
CuO from Cu-TEOA	780	--	30
CuO NW on Cu foil	485	580	39
annealed CuO	430	580	40
CuO from Cu-EA	370	475	This work

The chemical compositions and the valence states of the catalyst film were further examined by XPS (Figure 2b and Figure S2). The XPS survey spectrum reveals that the deposited materials mainly contain Cu, O, and C elements (Figure S2a) and the C 1s peak (285.0 eV) was used as the reference. The valence states of Cu and O elements were further probed by high-resolution XPS spectra of Cu 2p, Cu LMM, and O 1s. In the Cu 2p spectra (Figure 2b), obvious shake-up satellite peaks suggested that the oxidation state of Cu element is probably +2.²¹⁻²² Since both CuO and Cu(OH)₂ materials have similar Cu 2p_{3/2} character, it is necessary to further confirm the real source of Cu²⁺ by examining the Cu LMM spectrum. In the Cu LMM spectrum (Figure S2b), an obvious single peak located at 918.2 eV is observed, which is consistent with the fingerprint of CuO.^{22-23, 30} The high-resolution O 1s spectrum was also collected (Figure S2c) and the result further confirmed the +2 valence state of the electrodeposited Cu-based catalyst. One peak at 529.4 eV was probably from the oxygen element in CuO and another two peaks located at 530.8 eV and 532.3 eV are tentatively assigned to the chemisorbed hydroxyl oxygen and chemisorbed water molecules, as also reported in previous studies.^{23, 30} Therefore, the electrodeposited catalysts from **Cu-EA** precursor were identified as CuO materials. Grey film electrodeposited from **Cu-PA** precursor was also examined by XRD and XPS and the results are shown in

Figure S3, which exhibited nearly the same chemical compositions as the material obtained from **Cu-EA** precursor.

Figure 2c shows the SEM images of the electrodeposited CuO materials from **Cu-EA** complex on FTO after 3 hours of electrolysis. The CuO materials contains interlaced nanoblocks with a length of ~ 500 nm. It is worth mentioning that the surfaces of these nanoblocks are full of noticeable cracks which may help increase the surface area. The inset image in Figure 2c is the cross-section of the film, illustrating its thickness of ~ 780 nm after 3 hours of electrolysis. The morphology of electrodeposited CuO materials from **Cu-PA** was also provided in Figure S4. It is found that the material electrodeposited from **Cu-PA** has similar thickness to the materials obtained from **Cu-EA** precursor but shows more irregular nanostructure. Figure 2d shows a high-resolution TEM image of the CuO material obtained from **Cu-EA**, in which the phase distance between the adjacent lattice fringes is 0.252 nm, corresponding to the (-111) crystal plane of the standard CuO diffraction pattern (PDF #89-5895).

To further investigate the catalytic activities of the catalyst film for OER, linear sweep voltammograms (LSV) were performed in 1.0 M KOH solution (pH ~ 13.6) at a scan rate of 10 mV/s using the electrodeposited CuO film (electrodeposition at 0.8 V vs. Ag/AgCl for 3 h) from **Cu-EA** precursor as the working electrode. The black plot in Figure 3a is the control experiment using a bare FTO electrode and the red plot shows the LSV data of CuO film with no iR compensation. No obvious catalytic activity was observed from the control experiment at 1.2 V to 1.8 V vs. RHE. In contrast, the as-electrodeposited CuO film showed excellent catalytic activity for oxygen evolution in water. The overpotential to generate 10 mA/cm² for the present CuO film is only ~ 470 mV (1.70 V vs. RHE). To the best of our knowledge, this catalytic performance is much higher than other copper-based heterogeneous catalysts for water oxidation, as shown in Table 1.^{13, 21-25, 31} These results confirm that the electrodeposited CuO material is an active catalyst for water oxidation. Moreover, the influence of the iR compensation was studied and the LSV data obtained with 20% iR compensation are shown in Figure 3a (blue plot). When 20% iR compensation was applied, the curve for OER was much sharper than the catalytic plot without iR compensation and much higher catalytic current densities were obtained under the same applied potential. For example, to achieve a current density of 10 mA/cm², the applied working potential was ~ 1.65 V vs. RHE, which is less than the ~ 1.70 V (red plot) with no iR compensation.

The LSVs of the CuO films obtained from **Cu-PA** and **Cu-EA** precursors in 1.0 M KOH solution are compared in Figure S5. The results showed the CuO film deposited from **Cu-EA** has much better catalytic activity for OER than that obtained from **Cu-PA**. The roughness factor (RF) may explain the different OER performances in two CuO films, which was realized by measuring the CVs at various scan rates in the non-Faradaic region (Figure S6). Based on the results, C_{dl} of the CuO film from **Cu-EA** showed a much higher value than that from **Cu-PA** ($RF = C_{dl}/(C_s \cdot S_{geo})$, C_{dl} is the electrochemical double layer capacitance and C_s is specific electrochemical double layer capacitance of an atomically smooth surface). The higher value of C_{dl} in the CuO film from **Cu-EA** indicated a higher RF and further resulted in a higher performance toward OER. As the CuO material deposited from **Cu-EA** showed a better catalytic property, the following experiments are focused on this CuO film.

The catalytic stability of the as-deposited CuO material for OER was measured in galvanostatic electrolysis at 1.0 and 10 mA/cm² in

1.0 M KOH (Figure 3b). The results show that the catalytic overpotentials under different current densities exhibited no significant increase for 10 hours, suggesting good stability of the catalyst for OER catalysis. Consistent with the LSV results, the overpotentials for 1.0 and 10 mA/cm² were located at only ~ 370 mV and ~ 475 mV, respectively. Large amounts of gas bubbles were observed on the surface of the electrode, as seen in the inset picture in Figure 3b and the movie S1 for oxygen evolution provided in SI). In addition, the Tafel plot was obtained by measuring LSV at a scan rate of 2 mV/s in 1.0 M KOH (Figure 4a). The slope obtained from the plot is ~ 90 mV/dec for catalytic current densities from 1.0 mA/cm² to 10 mA/cm².

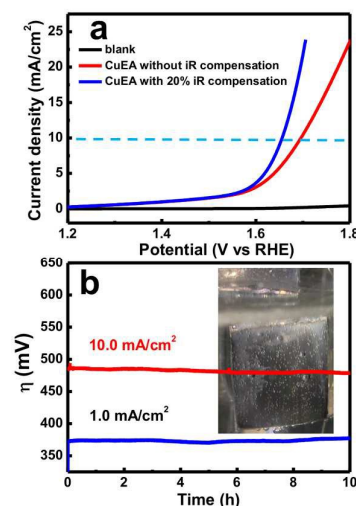


Figure 3. (a) Polarization curves for the CuO material electrodeposited from **Cu-EA** with 20% iR compensation (blue) and without iR compensation (red) in 1.0 M KOH buffer solution at pH 13.6. (b) Catalytic overpotential plots using the active CuO material under static current densities of 1.0 and 10 mA/cm² for 10 hours in 1.0 M KOH solution. Inset: oxygen bubbles on the surface of the CuO/FTO electrode.

The Faradaic efficiency was calculated based on the catalytic performance of the CuO thin film catalyst at 1.0 mA/cm² in a gas-tight electrochemical cell in 1.0 M KOH. The amount of evolved O₂ during OER over a certain period of electrolysis was measured by a fluorescence-based oxygen sensor. The experiment was performed for 4 hours and the corresponding plots are shown in Figure 4b. Oxygen was observed rapidly after initiating electrolysis and the amount of oxygen rose with the increase of passed charge. The theoretical yield of oxygen is calculated by assuming that all of the current was caused by 4e⁻ oxidation of water to produce oxygen. Comparing the experimental data with the theoretical data, the amount of oxygen evolved corresponds to a Faradaic yield which is > 95%.

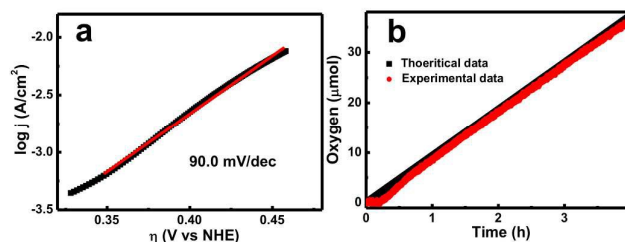


Figure 4. (a) The Tafel plot and (b) Faradic efficiency of oxygen production using the CuO thin film catalyst electrodeposited from **Cu-EA** in 1.0 M KOH solution.

After electrolysis for 10 hours, the surface composition and valence states of the CuO catalyst film material was probed again by XPS experiments. Figure S7a shows the Cu 2p spectra of the catalyst. Compared to the freshly electrodeposited CuO material, very similar shake-up satellite peaks and Cu 2p_{3/2} peaks were observed for the catalyst after OER catalysis and these peaks are consistent with the typical character of Cu²⁺ in CuO.^{21, 23, 30} In addition, the Cu LMM spectrum showed an obvious single peak located at 918.2 eV and further confirmed the durability of the CuO (Figure S7b).^{22-23, 30} XRD results for the CuO material after electrolysis showed nearly the same diffraction peaks as the fresh sample (PDF# 89-5895) and SnO₂ on FTO substrate (SnO₂ PDF# 77-0452) (Figure S7c). Therefore, after electrolysis, there still exists only pure CuO on the FTO electrode. Based on the above-mentioned XRD and XPS results, the present in situ generated CuO material is quite robust for OER catalysis.

Conclusions

In summary, our present study reports a simple one-step method to form highly active heterogeneous CuO catalyst in situ from Cu-EA complex for OER catalysis in alkaline conditions. The OER activity of the CuO catalyst showed a very low overpotential of only ~470 mV to achieve 10 mA/cm² in 1.0 M KOH at pH 13.6. This performance makes it one of the most efficient known copper-based heterogeneous catalyst for water oxidation. Furthermore, the electrodeposited CuO material is quite robust during water oxidation, as evidenced by XRD and XPS measurements after a long period of electrolysis. The simple synthesis method, low cost, and high activity of the present CuO thin film catalyst highlight its great potential as an efficient catalyst for future low-cost electrochemical water splitting devices.

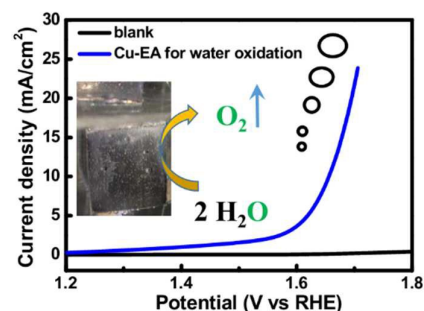
This work was financially supported by NSFC (21271166, 21473170), the Fundamental Research Funds for the Central Universities, the Program for New Century Excellent Talents in University (NCET), and the Thousand Young Talents Program.

Notes and references

- J. L. Dempsey, B. S. Brunschwig, J. R. Winkler, H. B. Gray, *Acc. Chem. Res.*, 2009, **42**, 1995-2004.
- P. Du, R. Eisenberg, *Energy Environ. Sci.*, 2012, **5**, 6012-6021.
- N. S. Lewis, D. G. Nocera, *Proc. Natl. Acad. Sci. U.S.A.*, 2006, **103**, 15729-15735.
- D. G. Nocera, *Acc. Chem. Res.*, 2012, **45**, 767-776.
- J. P. McEvoy, G. W. Brudvig, *Chem. Rev.*, 2006, **106**, 4455-4483.
- R. Tagore, R. H. Crabtree, G. W. Brudvig, *Inorg. Chem.*, 2008, **47**, 1815-1823.
- J. J. Concepcion, J. W. Jurss, M. K. Brennaman, P. G. Hoertz, A. O. T. Patrocinio, N. Y. M. Iha, J. L. Templeton, T. J. Meyer, *Acc. Chem. Res.*, 2009, **42**, 1954-1965.
- D. Gust, T. A. Moore, A. L. Moore, *Acc. Chem. Res.*, 2009, **42**, 1890-1898.
- G. C. Dismukes, R. Brimblecombe, G. A. N. Felton, R. S. Pryadun, J. E. Sheats, L. Spiccia, G. F. Swiegers, *Acc. Chem. Res.*, 2009, **42**, 1935-1943.

- M. W. Kanan, D. G. Nocera, *Science*, 2008, **321**, 1072-1075.
- V. Artero, M. Chavarot-Kerlidou, M. Fontecave, *Angew. Chem. Int. Ed.*, 2011, **50**, 7238-7266.
- M. Dincă, Y. Surendranath, D. G. Nocera, *Proc. Natl. Acad. Sci. U.S.A.*, 2010, **107**, 10337-10341.
- S. M. Barnett, K. I. Goldberg, J. M. Mayer, *Nat. Chem.*, 2012, **4**, 498-502.
- Z. F. Chen, T. J. Meyer, *Angew. Chem. Int. Ed.*, 2013, **52**, 700-703.
- M. T. Zhang, Z. F. Chen, P. Kang, T. J. Meyer, *J. Am. Chem. Soc.*, 2013, **135**, 2048-2051.
- W. C. Ellis, N. D. McDaniel, S. Bernhard, T. J. Collins, *J. Am. Chem. Soc.*, 2010, **132**, 10990-10991.
- M. Taki, S. Itoh, S. Fukuzumi, *J. Am. Chem. Soc.*, 2001, **123**, 6203-6204.
- L. M. Mirica, O. X. T. D. P. Stack, *Chem. Rev.*, 2004, **104**, 1013-1045.
- C. J. Cramer, W. B. Tolman, *Acc. Chem. Res.*, 2007, **40**, 601-608.
- P. Kang, E. Bobyr, J. Dustman, K. O. Hodgson, B. Hedman, E. I. Solomon, T. D. P. Stack, *Inorg. Chem.*, 2010, **49**, 11030-11038.
- X. Liu, H. Jia, Z. Sun, H. Chen, P. Xu, P. Du, *Electrochem. Commun.*, 2014, **46**, 1-4.
- X. Liu, S. Cui, Z. Sun, P. Du, *Electrochim. Acta*, 2015, **160**, 202-208.
- X. Liu, H. Zheng, Z. Sun, A. Han, P. Du, *ACS Catal.*, 2015, **5**, 1530-1538.
- F. Yu, F. Li, B. Zhang, H. Li, L. Sun, *ACS Catal.*, 2014, **5**, 627-630.
- T. T. Li, S. Cao, C. Yang, Y. Chen, X. J. Lv, W. F. Fu, *Inorg. Chem.*, 2015, **54**, 3061-3067.
- Y. J. Sa, K. Kwon, J. Y. Cheon, F. Kleitz, S. H. Joo, *J. Mater. Chem. A*, 2013, **1**, 9992-10001.
- L. Wu, Q. Li, C. H. Wu, H. Zhu, A. Mendoza-Garcia, B. Shen, J. Guo, S. Sun, *J. Am. Chem. Soc.*, 2015, **137**, 7071-7074.
- M. Dinca, Y. Surendranath, D. G. Nocera, *Proc. Natl. Acad. Sci. U.S.A.*, 2010, **107**, 10337-10341.
- A. Han, H. L. Chen, Z. J. Sun, J. Xu, P. Du, *Chem. Comm.*, 2015, **51**, 11626-11629.
- N. S. McIntyre, S. Sunder, D. W. Shoesmith, F. W. Stanchell, *J. Vac. Sci. Technol.*, 1981, **18**, 714-721.
- J. L. Du, Z. F. Chen, S. R. Ye, B. J. Wiley, T. J. Meyer, *Angew. Chem. Int. Ed.*, 2015, **54**, 2073-2078.

Table of contents



Journal Name

COMMUNICATION

Published on 16 March 2016. Downloaded by University of Florida on 17/03/2016 02:00:26.

ChemComm Accepted Manuscript